Proceedings of the 17th World Congress
The International Federation of Automatic Control
Seoul, Korea, July 6-11, 2008

Root Cause Diagnosis of Plant-wide Oscillations using the Adjacency Matrix

Hailei Jiang * **Rohit Patwardhan** ** **Sirish L. Shah** *,[1]

* *Department of Chemical and Materials Engineering, University of Alberta, Edmonton, AB, Canada, T6G 2G6*
** *Matrikon Inc., Suite 1800 10405 Jasper Avenue, Edmonton, Alberta, Canada T5J 3N4*

Abstract: Oscillations are a common type of plant-wide disturbances whose effects propagate to many units and thus may impact overall process performance. It is important to detect and diagnose such oscillations early in order to rectify the situation. Many frequency domain tools such as the power spectrum and spectrum envelope methods are capable of detecting the oscillation frequency. However, few methods are available for locating the root cause which is the main objective of oscillation diagnosis. This paper proposes a new method to diagnose the root cause of plant-wide oscillations using the adjacency matrix. A novel feature of the new method is that it utilizes the information in the process flowsheet. The method is not data-based and it can be carried out without using any data. However this method complements the data based methods very well and it is best used in combination with other data-based methods to provide powerful diagnosis of plant-wide oscillations. This paper is the subject of a newly proposed complete procedure for detection and diagnosis of plant-wide oscillation. Two industrial case studies are also presented to demonstrate the applicability of the proposed procedure.

Keywords: Digraph, Adjacency matrix, Oscillation, Fault Diagnosis,

1. INTRODUCTION

Oscillations are a common type of plant-wide disturbances. Their root causes can be poorly tuned controllers, process or actuator non-linearities, oscillatory disturbance *etc.* The effects of such oscillation can propagate to many units and thus may impact overall process performance of the plant. The presence of oscillations in a plant increases the variability of the process variables and thus may cause poor control performance, inferior quality products and larger rejection rates. For this reason the detection and diagnosis of plant-wide disturbances is an important issue in many process industries.

Many methods have been proposed in the literature for oscillation detection. Thornhill and Hägglund (1997) used zero-crossings of the control error signal to calculate integral absolute error (IAE) in order to detect oscillation in a control loop. Miao and Seborg (1999) suggested a method based on the auto-correlation function to detect excessively oscillatory feedback loops. The auto-covariance function (ACF) of a signal was utilized in Thornhill *et al.* (2003*a*) to detect oscillation(s) present in a signal. Thornhill *et al.* (2002) proposed spectral principal component analysis (SPCA) to detect oscillations and categorize all variables having similar oscillations. Most recently, Jiang *et al.* (2007) have utilized the spectral envelope method for oscillation detection.

However, the literature is relatively sparse on studies concerned with root cause diagnosis of plant-wide oscillations. Thornhill *et al.* (2001) and Thornhill *et al.* (2003*b*) proposed to calculate distortion factors and nonlinearity index of process variables and use them as an indication of possible root cause. Jiang *et al.* (2007) proposed an index defined as the Oscillation Contribution Index (OCI) to evaluate the severity of oscillation in each variable and its subsequent use as an indicator of potential root cause. All these methods are data-based and do not utilize process knowledge. The contribution of these data-based root cause diagnosis techniques is to isolate a few variables as the likely root cause candidates. Due to the complexity of large-scale plants and the difficulty of determining cause-effect relationship, it is difficult to conclude whether a certain variable is the root cause by only analyzing plant data.

In the recent years, graph-based approaches have been proposed by various researchers for safety analysis and fault diagnosis of chemical process systems (Maurya *et al.*, 2003*a*). Maurya *et al.* (2003*a*) and Maurya *et al.* (2003*b*) gave a comprehensive review of the signed digraph (SDG) and showed how to develop graph models systematically from a system of differential-algebraic equations. Yim *et al.* (2006) used process topology in plant-wide control performance assessment. They used the computer aided engineering exchange (CAEX) file to describe items of equipment in the plant, such as tanks, pipes, valves and instruments and how they are linked physically. Recently, Bauer *et al.* (2007) described a data-driven method for

[1] Corresponding author. Tel.:+1-780-492-5162;
fax:+1-780-492-2881.
E-mail address: sirish.shah@ualberta.ca

978-1-1234-7890-2/08/$20.00 © 2008 IFAC 10.3182/20080706-5-KR-1001.1970

identifying the direction of propagation of disturbance based on the concept of transfer entropy.

The main purpose of this paper is to incorporate process knowledge, such as process flowsheet or topology, control configuration and instrument information, into an oscillation diagnosis tool. We propose a novel way to convert a process schematic to a digraph based on the information of controllers. The new digraph is called *control loop digraph*. Then, the concept of adjacency matrix will be used to develop a process knowledge based method for oscillation diagnosis. Combination of this method with other data-based methods can provide a powerful diagnosis of root cause of plant-wide oscillations.

The remainder of this paper is organized as follows. Section 2 gives a brief introduction to the adjacency matrix and the reachability matrix. In Section 3, through an experimental example and an industrial case study, we show how to use the adjacency matrix and reachability matrix for oscillation diagnosis. In Section 4, we will summarize the complete procedure for oscillation detection and diagnosis, followed by a second industrial case study. The paper ends with concluding remarks in Section 5.

2. DIGRAPHS AND THE ADJACENCY MATRIX

A graph is a mathematical abstraction of structural relationships between discrete objects (Mah, 1989). The objects are represented by a set of *nodes*, and the existence of relationship between two objects is presented by *edges*. If a sense of direction is imparted to each edge of a graph, such a graph is called a *directed graph* or a *digraph* for short. Figure 1(a) shows a simple digraph where $\{a, b, c, d, e\}$ are nodes and the lines with arrow are edges. In graph theory, there are several methods to represent a digraph by a matrix. A common one is to represent a digraph by an *adjacency matrix* (Mah, 1989). In an adjacency matrix the rows and columns both represent the nodes. The (i, j)th entry is assigned a value of “1” if there is a directed edge from node i to node j, other wise it is assigned a value of “0”.

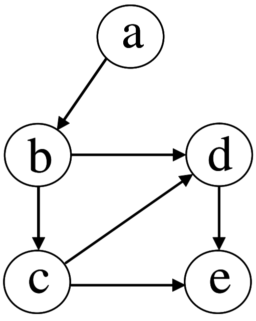

(a) A simple digraph

$$\begin{array}{c} \\ a \\ b \\ c \\ d \\ e \end{array}\begin{array}{c} \begin{matrix} a & b & c & d & e \end{matrix} \\ \begin{bmatrix} 0 & 1 & 0 & 0 & 0 \\ 0 & 0 & 1 & 1 & 0 \\ 0 & 0 & 0 & 1 & 1 \\ 0 & 0 & 0 & 0 & 1 \\ 0 & 0 & 0 & 0 & 0 \end{bmatrix} \end{array} = \mathbf{X}$$

(b) Adjacency matrix

Fig. 1. A digraph and its adjacency matrix

The adjacency matrix (denoted as $\mathbf{X}$) of the digraph in Figure 1(a) is shown in Figure 1(b). It is clear that the total number of “1”s in the adjacency matrix is given by the number of edges in the digraph. A very interesting and useful property of adjacency matrix is: the (i, j) element of $\mathbf{X}^k$ gives the number of k-step edge sequences from node i to node j. For example, the following matrices are successive powers of the adjacency matrix in Figure 1(b). By examining these matrices it is easy to verify the above mentioned property. For example, element $(2, 5)$ in $\mathbf{X}^2$ shows that there are two 2-step edge sequences from node b to node e; and as is clear from Figure 1(a) we can find that the two 2-step edge sequences from node b to node e as $\{b \to c \to e\}$ and $\{b \to d \to e\}$.

$$\mathbf{X}^2 = \begin{bmatrix} 0 & 0 & 1 & 1 & 0 \\ 0 & 0 & 0 & 1 & 2 \\ 0 & 0 & 0 & 0 & 1 \\ 0 & 0 & 0 & 0 & 0 \\ 0 & 0 & 0 & 0 & 0 \end{bmatrix} \quad \mathbf{X}^3 = \begin{bmatrix} 0 & 0 & 0 & 1 & 2 \\ 0 & 0 & 0 & 0 & 1 \\ 0 & 0 & 0 & 0 & 0 \\ 0 & 0 & 0 & 0 & 0 \\ 0 & 0 & 0 & 0 & 0 \end{bmatrix}$$

$$\mathbf{X}^4 = \begin{bmatrix} 0 & 0 & 0 & 0 & 1 \\ 0 & 0 & 0 & 0 & 0 \\ 0 & 0 & 0 & 0 & 0 \\ 0 & 0 & 0 & 0 & 0 \\ 0 & 0 & 0 & 0 & 0 \end{bmatrix} \quad \mathbf{X}^5 = \begin{bmatrix} 0 & 0 & 0 & 0 & 0 \\ 0 & 0 & 0 & 0 & 0 \\ 0 & 0 & 0 & 0 & 0 \\ 0 & 0 & 0 & 0 & 0 \\ 0 & 0 & 0 & 0 & 0 \end{bmatrix}$$

Before introducing the reachability matrix, we define the Boolean equivalent of any matrix $\mathbf{A}$ by the following relationship (Mah, 1989):

$$\mathbf{A}^{\#}(i, j) = \begin{cases} 0, & if \ \ \mathbf{A}(i, j) = 0 \\ 1, & if \ \ \mathbf{A}(i, j) \neq 0 \end{cases} \tag{1}$$

For a digraph with N nodes and an adjacency matrix $\mathbf{X}$, the following matrix

$$\mathbf{R} = (\mathbf{X} + \mathbf{X}^2 + \mathbf{X}^3 + ... + \mathbf{X}^N)^{\#} \tag{2}$$

is defined as the reachability matrix (Mah, 1989). The (i, j)th element of $\mathbf{R}$ indicates whether there exists any directed path of any length whatsoever from node i to node j. The reachability matrix for the digraph in Figure 1(a) is

$$\mathbf{R} = \begin{bmatrix} 0 & 1 & 1 & 1 & 1 \\ 0 & 0 & 1 & 1 & 1 \\ 0 & 0 & 0 & 1 & 1 \\ 0 & 0 & 0 & 0 & 1 \\ 0 & 0 & 0 & 0 & 0 \end{bmatrix}$$

The reachability matrix provides a conceptually simple and direct method of determining the connectivity of a digraph (Mah, 1989). For instance, the entries in $\mathbf{R}$ show that node a can reach all the other nodes, but node a can not be reached from any other node. Similarly, node b can reach $\{c, d, e\}$, but not vice versa.

3. CONTROL LOOP DIGRAPH BASED ON PROCESS FLOWSHEET

The idea of *process digraph* in Mah (1989) is to denote units, tanks and junctions of a process as nodes and physical connections as edges in a digraph. This process digraph is used for design of continuous processes and in the treatment of batch plant scheduling and design. However, this equipment-based process digraph is not appropriate for oscillation diagnosis where control loops also need to be considered. In this section, we introduce the concept of *control loop digraph* for oscillation analysis.

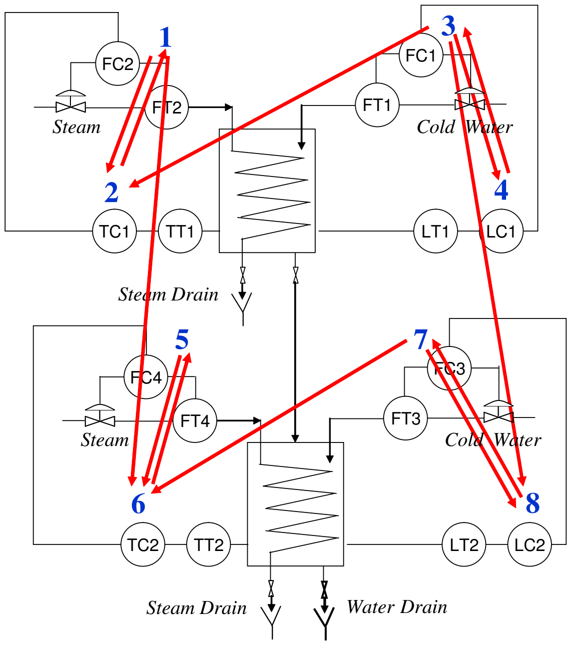

Fig. 2. Control loop digraph of a two-tank system

		1 FC2	2 TC1	3 FC1	4 LC1	5 FC4	6 TC2	7 FC3	8 LC2
1	FC2	1	1	0	0	0	1	0	0
2	TC1	1	1	0	0	0	0	0	0
3	FC1	0	1	1	1	0	0	0	1
4	LC1	0	0	1	1	0	0	0	0
5	FC4	0	0	0	0	1	1	0	0
6	TC2	0	0	0	0	1	1	0	0
7	FC3	0	0	0	0	0	1	1	1
8	LC2	0	0	0	0	0	0	1	1

Fig. 3. Adjacency matrix of the two-tank system

		1 FC2	2 TC1	3 FC1	4 LC1	5 FC4	6 TC2	7 FC3	8 LC2
1	FC2	1	1	0	0	1	1	0	0
2	TC1	1	1	0	0	1	1	0	0
3	FC1	1	1	1	1	1	1	1	1
4	LC1	1	1	1	1	1	1	1	1
5	FC4	0	0	0	0	1	1	0	0
6	TC2	0	0	0	0	1	1	0	0
7	FC3	0	0	0	0	1	1	1	1
8	LC2	0	0	0	0	1	1	1	1

Fig. 4. Reachability matrix of the two-tank system

3.1 Control Loop Digraph

As mentioned earlier, because of feedback and/or feedforward control and other physical connections in a process, an oscillation often starts from a single loop and propagates to other loops. To build and analyze the digraph of a process from a control plus process flowsheet perspective we denote each controller in a process schematic as a node. Next we use a concept of *direct interaction* to add edges between the nodes. We define a direct interaction from node i to node j if the controller output of controller i ($i.OP$) can directly affect the controlled variable of controller j ($j.PV$) without going through controller output of any other nodes; and we can add an edge from node i to node j in the process flowsheet. To achieve a complete analysis of direct interactions in a plant, we utilize all information of the control structure and process flowsheet connections. With controllers as nodes, and direct interactions as edges, we propose a new digraph that we define as a *control loop digraph*. The following example illustrates how to create a control loop digraph from a process flowsheet.

3.2 Example

Figure 2 shows a two-tank system where FT, LT, FC and LC represent flow transmitter, level transmitter, flow controller and level controller respectively. The outlet water from the upper tank flows directly into the lower tank. For each tank there is a cascaded temperature loop and also a level cascade loop. There are total of eight controllers in this system and these controllers are assigned a number from 1 to 8 separately as shown in Figure 2. The red lines with arrows represent the direct interactions between the controllers. For example, node 1 (FC2) has direct interactions with node 2 (TC1) and node 6 (TC2). This is because the OP of node 1 (FC2) can change the steam flowrate and therefore can affect the temperature of the upper tank (which is the PV of node 2, TC1); the temperature of the lower tank (which is the PV of node 6, TC2) can also be affected by the water from upper tank. Please notice that there is no direct interaction from node 1 (FC2) to node 5 (FC4). This is because the OP of node 1 can only affect the PV of node 5 through the OP of node 6 (TC2). If node 5 (FC4) is not cascaded with node 6 (TC2), then node 1 can not affect node 5. Therefore we say there is no direct interaction from node 1 to node 5. Following the definition of direct interaction, we can obtain a complete analysis of the two-tank system and come up with the control loop digraph shown in Figure 2.

The adjacency matrix of the control loop digraph of the two-tank system is shown in Figure 3 which is different from the concept we introduced in Section 2. In section 2, we did not put "1" on the diagonal, but here we have assigned "1" on the diagonal which means that the OP of a controller will affect the PV of itself first. The

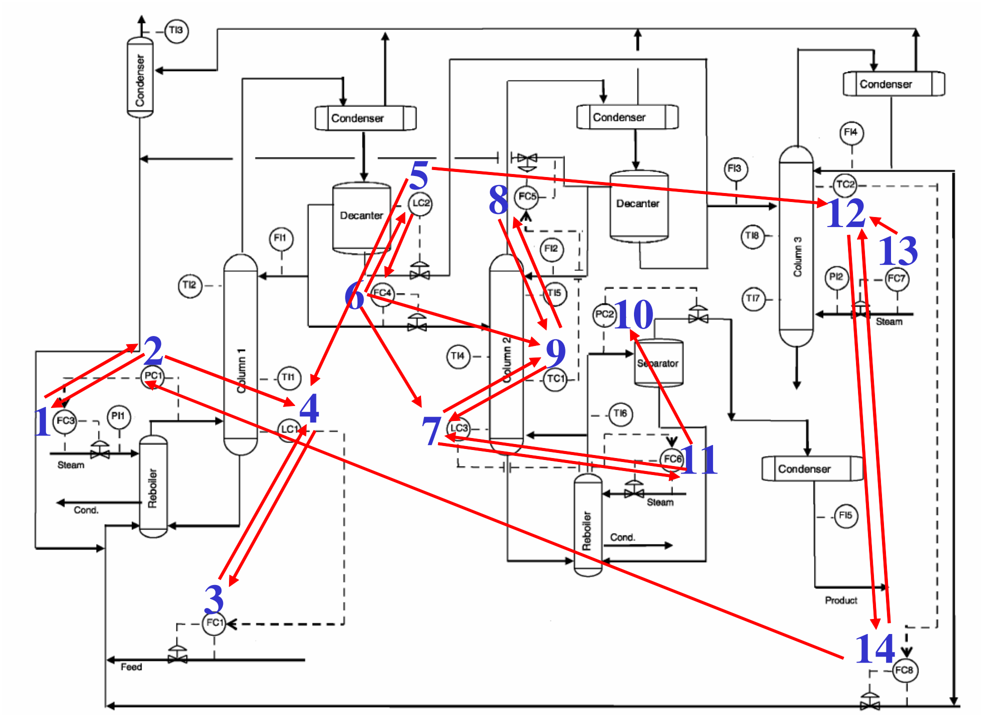

Fig. 5. Control-based process digraph of a process from Eastman Chemical Company, USA

		1 FC3	2 PC1	3 FC1	4 LC1	5 LC2	6 FC4	7 LC3	8 FC5	9 TC1	10 PC2	11 FC6	12 TC2	13 FC7	14 FC8
1	FC3	1	1	0	0	0	0	0	0	0	0	0	0	0	0
2	PC1	1	1	0	1	0	0	0	0	0	0	0	0	0	0
3	FC1	0	0	1	1	0	0	0	0	0	0	0	0	0	0
4	LC1	0	0	1	1	0	0	0	0	0	0	0	0	0	0
5	LC2	0	0	0	1	1	1	0	0	0	0	0	1	0	0
6	FC4	0	0	0	0	1	1	1	0	1	0	0	0	0	0
7	LC3	0	0	0	0	0	0	1	0	1	0	1	0	0	0
8	FC5	0	0	0	0	0	0	0	1	1	0	0	0	0	0
9	TC1	0	0	0	0	0	0	1	1	1	0	0	0	0	0
10	PC2	0	0	0	0	0	0	0	0	0	1	0	0	0	0
11	FC6	0	0	0	0	0	0	1	0	0	1	1	0	0	0
12	TC2	0	0	0	0	0	0	0	0	0	0	0	1	0	1
13	FC7	0	0	0	0	0	0	0	0	0	0	0	1	1	0
14	FC8	0	1	0	0	0	0	0	0	0	0	0	1	0	1

(a) Adjacency matrix

		1 FC3	2 PC1	3 FC1	4 LC1	5 LC2	6 FC4	7 LC3	8 FC5	9 TC1	10 PC2	11 FC6	12 TC2	13 FC7	14 FC8
1	FC3	1	1	1	1	0	0	0	0	0	0	0	0	0	0
2	PC1	1	1	1	1	0	0	0	0	0	0	0	0	0	0
3	FC1	0	0	1	1	0	0	0	0	0	0	0	0	0	0
4	LC1	0	0	1	1	0	0	0	0	0	0	0	0	0	0
5	LC2	1	1	1	1	1	1	1	1	1	1	1	1	0	1
6	FC4	1	1	1	1	1	1	1	1	1	1	1	1	0	1
7	LC3	0	0	0	0	0	0	1	1	1	1	1	0	0	0
8	FC5	0	0	0	0	0	0	1	1	1	1	1	0	0	0
9	TC1	0	0	0	0	0	0	1	1	1	1	1	0	0	0
10	PC2	0	0	0	0	0	0	0	0	0	1	0	0	0	0
11	FC6	0	0	0	0	0	0	1	1	1	1	1	0	0	0
12	TC2	1	1	1	1	0	0	0	0	0	0	0	1	0	1
13	FC7	1	1	1	1	0	0	0	0	0	0	0	1	1	1
14	FC8	1	1	1	1	0	0	0	0	0	0	0	1	0	1

(b) Reachability matrix

Fig. 6. Adjacency matrix and reachability matrix of the Eastman Process shown in Figure 5

corresponding reachability matrix is shown in Figure 4. It is clear in Figure 4 that node 3 (FC1) and node 4 (LC1) can reach (or affect) all the other controllers in the two-tank system. This observation is consistent with our expectation that the water flow rate to the upper tank and the level of upper tank can affect the PVs of all other controllers. Additionally, we can see in Figure 4 that nodes 5-8 can not reach node 1-4. This means that the controllers of lower tank can not affect the controllers of upper tank which also concurs with the real situation. We can also conclude from the reachability matrix that the temperature cascade loops (nodes 1&2 and nodes 5&6) can not affect the level cascade loops (nodes 3&4 and nodes 7&8). These results do confirm that the control loop digraph (based on direct interactions) and its corresponding reachability matrix can correctly represent the interactions in a process.

3.3 Industrial Application for Oscillation Diagnosis

Figure 5 shows an schematic of a process at Eastman Chemical Company, USA. In this case study (also for the case study in Section 4), AC, FC, LC, PC and TC represent composition, flow, level, pressure and temperature tags, respectively, that are controlled. Similarly, FI, LI, PI, TI and SI represent the flow, level, pressure, temperature and rotor speed tags, respectively, that are indicators only. There are 14 PID controllers in this process. To draw the control loop digraph of this process, we take the controllers as nodes and consider the direct interactions between different nodes. For example, node 1 and node 2 are the secondary and the master controllers in a cascade control loop. Either the OP of node 1 or node 2 moves, the PV of other node will be affected. Therefore, we say nodes 1 and 2 have direct interactions between them and we add edges between nodes 1 and 2. After a complete analysis of direct interactions, we can draw the control loop digraph of this process as shown in Figure 5. The adjacency matrix of the digraph is shown in Figure 6(a). The corresponding reachability matrix is shown in Figure 6 which shows that nodes 5 and 6 have connections to all the other nodes except node 13.

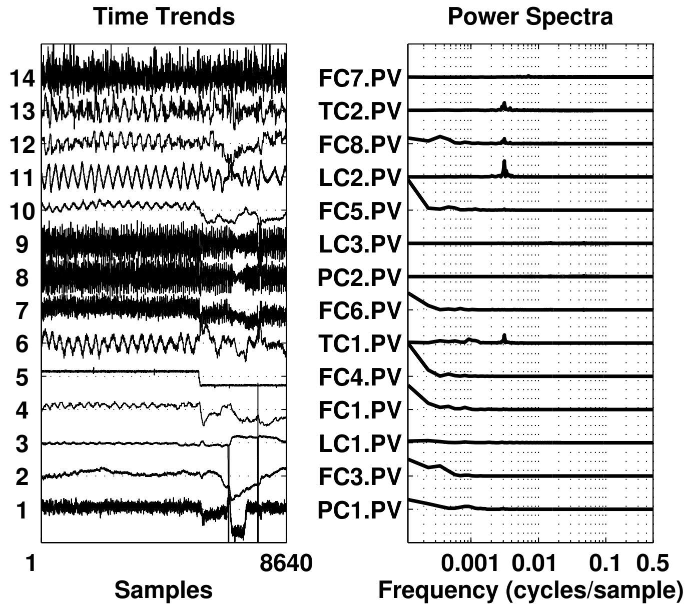

Fig. 7. Time trend and power spectra of 14 *pv*'s

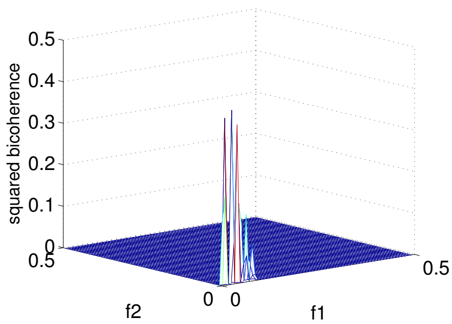

(a) Bicoherence Plot

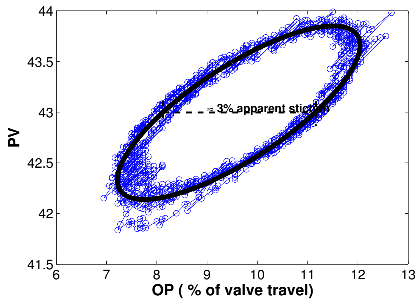

(b) LC2 $pv - op$ plot

Fig. 8. Oscillation diagnosis for LC2loop

3.4 Oscillation diagnosis

The Advanced Controls Technology group of Eastman Chemical Company had noticed that many of the process variables in this particular unit were oscillating and they needed to find out the root cause of these oscillations. Figure 7 shows the time trends and power spectra of the 14 *pv* variables. The sampling time of the time trends is 1 minute. The power spectra indicate the presence of oscillation at the frequency of 0.003 cycles/sample (or about 333 samples/cycle, nearly a period of 2 hours). This oscillation had propagated through out the adjacent units and affected many variables in the process.

In an earlier study, Jiang *et al.* (2007) have used the spectral envelope method to detect the oscillation frequencies and isolate all the variables that were oscillating at the same frequency of concern. In Figure 6, the variables highlighted in blue are the variables oscillating at the frequency of concern (Jiang *et al.*, 2007).

The diagnosis that we arrive at based on the reachability matrix is that: if the oscillation started from one loop in the process, then the root cause must be either loops 5 or 6 because these are the only two loops that can reach all the detected oscillatory loops. The root cause of an oscillatory signal can be many: tight tuning of the control loop, or an oscillatory disturbance or process or valve non-linearity. After further investigation it was determined that valve stiction related limit cycles was a likely source of the oscillatory signal in one of these loops. Choudhury *et al.* (2004), Choudhury *et al.* (2006) used bicoherence and $pv - op$ plot to detect and diagnose valve stiction. We followed their method and Figure 8 shows the bicoherence plot and the $pv - op$ plot of loop 5. The presence of large bicoherence value and an ellipse in the $pv - op$ plot is a clear evidence of valve stiction in loop 5; we did not find valve stiction in loop 6. Therefore our analysis indicating loop 5 (LC2) is the root cause. Now, plant tests have confirmed that the control valve of LC 2 is truly the root cause and caused other variables to oscillate (Thornhill *et al.*, 2003*b*).

4. OSCILLATION DETECTION AND DIAGNOSIS

In the previous section, we introduced the concept of control loop digraph and used its adjacency matrix and reachability matrix to diagnose the root cause of plant-wide oscillations. A novel feature of this method is that it

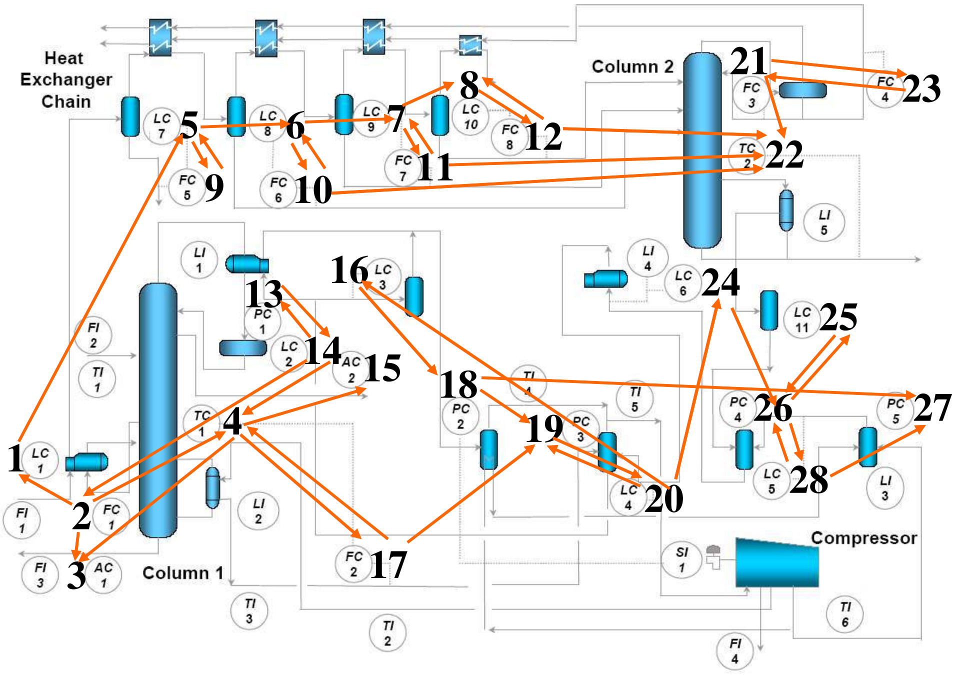

Fig. 9. Control loop digraph of a process from Mitsubishi Chemical Corporation, Japan

is not data-based. A combination of this method and other data-based methods can provide an effective detection and diagnosis tool. Next we summarize the newly proposed complete and comprehensive procedure for oscillation detection and diagnosis:

(1) Use frequency domain methods, such as spectral envelope and power spectral to detect loops with common oscillations and their frequencies.

(2) Use the method presented in the previous section for oscillation diagnosis.

(3) To further confirm the diagnosis result from step (2), other methods for checking controller tuning, disturbance detection or detection of valve stiction, process nonlinearity can be used.

To show the effectiveness of the above procedure, we present one more industrial case study for the detection and diagnosis of plant-wide oscillations. An industrial data set was provided by the courtesy of Mitsubishi Chemical Corporation (MCC), Mizushima, Japan. Figure 9 shows the process schematic and the control loop digraph of the plant. The plant personnel reported oscillations with a period of about 2 $\sim$ 3 hours through out the plant, causing sub-optimal operation and large economic losses. The newly proposed procedure is applied to this large data set to detect and diagnose the cause of these plant-wide oscillations.

4.1 Oscillation Detection

We refer to Jiang *et al.* (2007) for results of oscillation detection. Jiang *et al.* (2007) used the spectral envelope method to detect the oscillation frequency and the oscillatory control loops. Here we give a summary of the result from Jiang *et al.* (2007): among the total of 28 loops, 19 loops were identified as having oscillations with a period of 144 mins. The variables that were oscillating at these frequency are listed in the following table.

Table 1. The loops that have oscillations

2 FC1	3 AC1	4 TC1	6 LC8	7 LC9	9 FC5	10 FC6
11 FC7	13 PC1	14 LC2	15 AC2	17 FC2	18 PC2	19 PC3
20 LC4	22 TC2	24 LC6	26 PC4	28 LC5		

4.2 Root Cause Diagnosis

After detecting the loops that have oscillation, the next objective was to locate the root cause in order to rectify the situation. First, considering direct interactions, we built the adjacency matrix from the control loop digraph. The adjacency matrix is shown in Figure 10. Then we built the reachability matrix from the adjacency matrix as shown in Figure 11. In Figure 11, the oscillatory variables listed in table 1 are highlighted in blue. It is clear that, if the oscillation started from a single loops in this process, then it must be either loop 13 (PC1) or loop 14 (LC2) because these are the only two loops that can reach all the oscillatory variables. As shown in Figure 9, these two loops are physically very close and both work for the same unit. Thus we isolate these two loops as root cause candidates.

4.3 Valve Stiction Detection

After narrowing down our focus to loops 13 and 14 from the total 28 loops, we would use other data-based methods to support our analysis. Choudhury *et al.* (2004), Choudhury *et al.* (2006) used bicoherence and $pv - op$ plot to detect and diagnose valve stiction. We followed their

		1 LC1	2 FC1	3 AC1	4 TC1	5 LC7	6 LC8	7 LC9	8 LC10	9 FC5	10 FC6	11 FC7	12 FC8	13 PC1	14 LC2	15 AC2	16 LC3	17 FC2	18 PC2	19 PC3	20 LC4	21 FC3	22 TC2	23 FC4	24 LC6	25 LC11	26 PC4	27 PC5	28 LC5
1	LC1	1	0	0	0	1	0	0	0	0	0	0	0	0	0	0	0	0	0	0	0	0	0	0	0	0	0	0	0
2	FC1	1	1	1	1	0	0	0	0	0	0	0	0	0	0	0	0	0	0	0	0	0	0	0	0	0	0	0	0
3	AC1	0	0	1	0	0	0	0	0	0	0	0	0	0	0	0	0	0	0	0	0	0	0	0	0	0	0	0	0
4	TC1	0	0	1	1	0	0	0	0	0	0	0	0	0	0	1	0	1	0	0	0	0	0	0	0	0	0	0	0
5	LC7	0	0	0	0	1	1	0	0	1	0	0	0	0	0	0	0	0	0	0	0	0	0	0	0	0	0	0	0
6	LC8	0	0	0	0	0	1	1	0	0	1	0	0	0	0	0	0	0	0	0	0	0	0	0	0	0	0	0	0
7	LC9	0	0	0	0	0	0	1	1	0	0	1	0	0	0	0	0	0	0	0	0	0	0	0	0	0	0	0	0
8	LC10	0	0	0	0	0	0	0	1	0	0	0	1	0	0	0	0	0	0	0	0	0	0	0	0	0	0	0	0
9	FC5	0	0	0	0	1	0	0	0	1	0	0	0	0	0	0	0	0	0	0	0	0	0	0	0	0	0	0	0
10	FC6	0	0	0	0	0	1	0	0	0	1	0	0	0	0	0	0	0	0	0	0	0	1	0	0	0	0	0	0
11	FC7	0	0	0	0	0	0	1	0	0	0	1	0	0	0	0	0	0	0	0	0	0	1	0	0	0	0	0	0
12	FC8	0	0	0	0	0	0	0	1	0	0	0	1	0	0	0	0	0	0	0	0	0	1	0	0	0	0	0	0
13	PC1	0	0	0	0	0	0	0	0	0	0	0	0	1	1	0	0	0	0	0	0	0	0	0	0	0	0	0	0
14	LC2	0	1	0	1	0	0	0	0	0	0	0	0	1	1	0	0	0	0	0	0	0	0	0	0	0	0	0	0
15	AC2	0	0	0	0	0	0	0	0	0	0	0	0	0	0	1	0	0	0	0	0	0	0	0	0	0	0	0	0
16	LC3	0	0	0	0	0	0	0	0	0	0	0	0	0	0	0	1	0	1	0	0	0	0	0	0	0	0	0	0
17	FC2	0	0	0	1	0	0	0	0	0	0	0	0	0	0	0	0	1	0	1	0	0	0	0	0	0	0	0	0
18	PC2	0	0	0	0	0	0	0	0	0	0	0	0	0	0	0	0	0	1	1	0	0	0	0	0	0	0	1	0
19	PC3	0	0	0	0	0	0	0	0	0	0	0	0	0	0	0	0	0	0	1	1	0	0	0	0	0	0	0	0
20	LC4	0	0	0	0	0	0	0	0	0	0	0	0	0	0	0	1	0	0	1	1	0	0	0	1	0	0	0	0
21	FC3	0	0	0	0	0	0	0	0	0	0	0	0	0	0	0	0	0	0	0	0	1	1	1	0	0	0	0	0
22	TC2	0	0	0	0	0	0	0	0	0	0	0	0	0	0	0	0	0	0	0	0	0	1	0	0	0	0	0	0
23	FC4	0	0	0	0	0	0	0	0	0	0	0	0	0	0	0	0	0	0	0	0	1	0	1	0	0	0	0	0
24	LC6	0	0	0	0	0	0	0	0	0	0	0	0	0	0	0	0	0	0	0	0	0	0	0	1	0	1	0	0
25	LC11	0	0	0	0	0	0	0	0	0	0	0	0	0	0	0	0	0	0	0	0	0	0	0	0	1	1	0	0
26	PC4	0	0	0	0	0	0	0	0	0	0	0	0	0	0	0	0	0	0	0	0	0	0	0	0	1	1	0	1
27	PC5	0	0	0	0	0	0	0	0	0	0	0	0	0	0	0	0	0	0	0	0	0	0	0	0	0	0	1	0
28	LC5	0	0	0	0	0	0	0	0	0	0	0	0	0	0	0	0	0	0	0	0	0	0	0	0	0	1	1	1

Fig. 10. Adjacency matrix of the digraph in Fig.9

		1 LC1	2 FC1	3 AC1	4 TC1	5 LC7	6 LC8	7 LC9	8 LC10	9 FC5	10 FC6	11 FC7	12 FC8	13 PC1	14 LC2	15 AC2	16 LC3	17 FC2	18 PC2	19 PC3	20 LC4	21 FC3	22 TC2	23 FC4	24 LC6	25 LC11	26 PC4	27 PC5	28 LC5
1	LC1	1	0	0	0	1	1	1	1	1	1	1	1	0	0	0	0	0	0	0	0	0	1	0	0	0	0	0	0
2	FC1	1	1	1	1	1	1	1	1	1	1	1	1	0	0	1	1	1	1	1	1	0	1	0	1	1	1	1	1
3	AC1	0	0	1	0	0	0	0	0	0	0	0	0	0	0	0	0	0	0	0	0	0	0	0	0	0	0	0	0
4	TC1	0	0	1	1	0	0	0	0	0	0	0	0	0	0	1	1	1	1	1	1	0	0	0	1	1	1	1	1
5	LC7	0	0	0	0	1	1	1	1	1	1	1	1	0	0	0	0	0	0	0	0	0	1	0	0	0	0	0	0
6	LC8	0	0	0	0	0	1	1	1	0	1	1	1	0	0	0	0	0	0	0	0	0	1	0	0	0	0	0	0
7	LC9	0	0	0	0	0	0	1	1	0	0	1	1	0	0	0	0	0	0	0	0	0	1	0	0	0	0	0	0
8	LC10	0	0	0	0	0	0	0	1	0	0	0	1	0	0	0	0	0	0	0	0	0	1	0	0	0	0	0	0
9	FC5	0	0	0	0	1	1	1	1	1	1	1	1	0	0	0	0	0	0	0	0	0	1	0	0	0	0	0	0
10	FC6	0	0	0	0	0	1	1	1	0	1	1	1	0	0	0	0	0	0	0	0	0	1	0	0	0	0	0	0
11	FC7	0	0	0	0	0	0	1	1	0	0	1	1	0	0	0	0	0	0	0	0	0	1	0	0	0	0	0	0
12	FC8	0	0	0	0	0	0	0	1	0	0	0	1	0	0	0	0	0	0	0	0	0	1	0	0	0	0	0	0
13	PC1	1	1	1	1	1	1	1	1	1	1	1	1	1	1	1	1	1	1	1	1	0	1	0	1	1	1	1	1
14	LC2	1	1	1	1	1	1	1	1	1	1	1	1	1	1	1	1	1	1	1	1	0	1	0	1	1	1	1	1
15	AC2	0	0	0	0	0	0	0	0	0	0	0	0	0	0	1	0	0	0	0	0	0	0	0	0	0	0	0	0
16	LC3	0	0	0	0	0	0	0	0	0	0	0	0	0	0	0	1	0	1	1	1	0	0	0	1	1	1	1	1
17	FC2	0	0	1	1	0	0	0	0	0	0	0	0	0	0	1	1	1	1	1	1	0	0	0	1	1	1	1	1
18	PC2	0	0	0	0	0	0	0	0	0	0	0	0	0	0	0	1	0	1	1	1	0	0	0	1	1	1	1	1
19	PC3	0	0	0	0	0	0	0	0	0	0	0	0	0	0	0	1	0	1	1	1	0	0	0	1	1	1	1	1
20	LC4	0	0	0	0	0	0	0	0	0	0	0	0	0	0	0	1	0	1	1	1	0	0	0	1	1	1	1	1
21	FC3	0	0	0	0	0	0	0	0	0	0	0	0	0	0	0	0	0	0	0	0	1	1	1	0	0	0	0	0
22	TC2	0	0	0	0	0	0	0	0	0	0	0	0	0	0	0	0	0	0	0	0	0	1	0	0	0	0	0	0
23	FC4	0	0	0	0	0	0	0	0	0	0	0	0	0	0	0	0	0	0	0	0	1	1	1	0	0	0	0	0
24	LC6	0	0	0	0	0	0	0	0	0	0	0	0	0	0	0	0	0	0	0	0	0	0	0	1	1	1	1	1
25	LC11	0	0	0	0	0	0	0	0	0	0	0	0	0	0	0	0	0	0	0	0	0	0	0	0	1	1	1	1
26	PC4	0	0	0	0	0	0	0	0	0	0	0	0	0	0	0	0	0	0	0	0	0	0	0	0	1	1	1	1
27	PC5	0	0	0	0	0	0	0	0	0	0	0	0	0	0	0	0	0	0	0	0	0	0	0	0	0	0	1	0
28	LC5	0	0	0	0	0	0	0	0	0	0	0	0	0	0	0	0	0	0	0	0	0	0	0	0	1	1	1	1

Fig. 11. Reachability matrix of the digraph in Fig.9

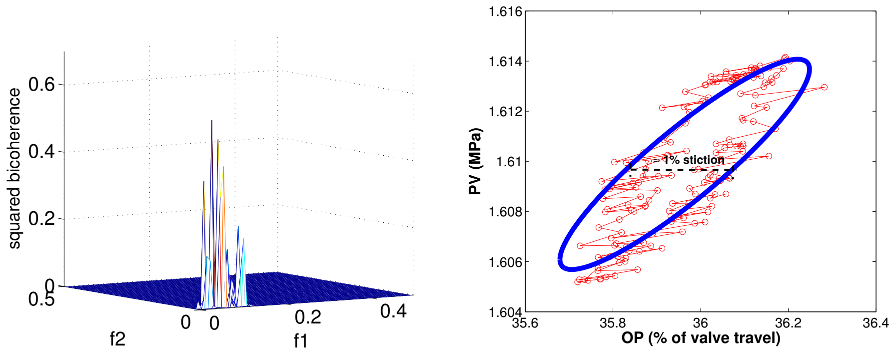

(a) Bicoherence Plot

(b) LC2 $pv - op$ plot

Fig. 12. Oscillation diagnosis for LC2loop

method to diagnose whether there is valve stiction in loop 13 or loop 14. Figure 12(a) shows the bicoherence plot and Figure 12(b) shows the $pv - op$ plot of loop 14 (PC1). The presence of large bicoherence value and an ellipse in the $pv - op$ plot is a clear evidence of valve stiction in loop 14.

We did not find valve stiction in loop 13. Therefore, our analysis confirmed that loop 14 (PC1) is the root cause. Further plant tests have confirmed that this loop with a sticky valve was indeed the leading cause of the plant-wide oscillations.

5. CONCLUDING REMARKS

In this paper, the concepts of adjacency matrix and reachability matrix have been reviewed. Based on these concepts, a new method for diagnosis of root cause of plant-wide oscillations is proposed. This method is not data-based and it can be carried out without using any data. Combination of this method and other data-based methods provides a complete procedure for detection and diagnosis of plant-wide oscillations. Two industrial case studies are presented to demonstrate the efficacy of the new procedure.

6. ACKNOWLEDGEMENT

The authors are grateful for the financial support from the Natural Sciences and Engineering Research Council of Canada, Matrikon Inc., Suncor Energy Inc. and Informatics Circle of Research Excellence, through the NSERC-Matrikon-Suncor-iCORE Senior Industrial Research Chair program at the University of Alberta.

The authors also thank Eastman Chemical Company and Mitsubishi Chemical Corporation for providing the data in this study.

REFERENCES

Bauer, Margret, John W. Cox, Michelle H. Caveness, James J. Downs and Nina F. Thornhill (2007). Finding the direction of disturbance propagation in a chemical process using transfer entropy. *IEEE transactions on control systems technology* **15**, 12–20.

Choudhury, M. A. A. S., S. L. Shah and N. F. Thornhill (2004). Diagnosis of poor control loop performance using higher order statistics. *Automatica* **40**(10), 1719–1728.

Choudhury, M. A. A. S., S. L. Shah, N. F. Thornhill and David S. Shook (2006). Automatic detection and quantification of stiction in control valves. *Control Engineering Practice* **14**, 1395–1412.

Jiang, Hailei, M. A. A. S. Choudhury and Sirish L. Shah (2007). Detection and diagnosis of plant-wide oscillations from industrial data using the spectral envelope method. *Journal of Process Control* **17**, 143–155.

Mah, Richard S.H. (1989). *Chemical Process Structures and Information Flows*. Butterworth Publishes.

Maurya, Mano Ram, Raghunathan Rengaswamy and Venkat Venkatasubramanian (2003*a*). A system framework for the development and analysis of signed digraphs for chemical processes. 1. algorithms and analysis. *Ind. Eng. Chem. Res.* **42**, 4789–4810.

Maurya, Mano Ram, Raghunathan Rengaswamy and Venkat Venkatasubramanian (2003*b*). A system framework for the development and analysis of signed digraphs for chemical processes. 2. control loops and flowsheet analysis. *Ind. Eng. Chem. Res.* **42**, 4811–4827.

Miao, T. and D.E. Seborg (1999). Automatic detection of excessive oscillatory feedback control loops. In: *Proc. of IEEE international Conference on Control Applications*. Kohala Coast, Hawai'i.

Thornhill, N.F. and T. Hägglund (1997). Detection and diagnosis of oscillation in control loops. *Control Engineering Practice*.

Thornhill, N.F., B. Huang and H. Zhang (2003*a*). Detection of multiple oscillations in control loops. *Journal of Process Control* **13**, 91–100.

Thornhill, N.F., John W. Cox and Michael A. Paulonis (2003*b*). Diagnosis of plant-wide oscillation through data-driven analysis and process understanding. *Control Engineering Practice* **11**, 1481–1490.

Thornhill, N.F., S.L. Shah and B. Huang (2001). Detection of distributed oscillations and root-cause diagnosis. In: *Proc. of CHEMFAS 4*. Jejudo Island, Korea. pp. 167–172.

Thornhill, N.F., S.L. Shah, B. Huang and A. Vishnubhotla (2002). Spectral principal component analysis of dynamic process data. *Control Engineering Practice* **10**, 833–846.

Yim, S.Y., H.G. Ananthankumar, L. Benabbs, A. Horch, R. Drath and N.F. Thornhill (2006). Using process topology in plant-wide control loop performance assessment. *Computers & Chemical Engineering* **31**, 89–99.